separations

MDPI

Article

Recovery of Bioactive Extracts from *Cistus creticus* Using Supercritical CO_2

Maria Chiliou, Vasiliki Louli and Kostis Magoulas *

Laboratory of Thermodynamics and Transport Phenomena, School of Chemical Engineering, National Technical University of Athens (NTUA), Zografou Campus, 15780 Athens, Greece; chilioumaria@gmail.com (M.C.); svlouli@chemeng.ntua.gr (V.L.)

* Correspondence: mag@chemeng.ntua.gr; Tel.: +30-210-772-3152

Abstract

Cistus creticus is a species of the Cistus family that exhibits a wide range of bioactivities; therefore, its oil recovery using a green extraction method is of significant importance for both academic research and industrial applications. Thus, the objective of this work is cistus oil recovery by supercritical fluid extraction (SFE) with CO_2. To this end, the effect of various process parameters, namely extraction pressure (110–250 bar), extraction temperature (40–60 °C), and solvent flow rate (1–3 kg/h), on the yield of the process was examined. It was shown that an increase in temperature, and particularly in pressure, positively affects the yield, while the flow rate increase mainly enhances the extraction rate. Hence, the highest yield (8.58% wt) was obtained at 60 °C, 250 bar, and 3 kg/h after 150 min of extraction. Furthermore, the experimental data regarding the kinetics of SFE were correlated successfully by a mass balance model based on Lack's plug flow model. In addition, the comparison of SFE extracts obtained under intermediate conditions with the essential oil produced by hydrodistillation revealed the extraction of heavier compounds, notably a high content of linoleic acid. Finally, the addition of a small amount of co-solvent (5% wt ethanol) to the SFE process enhanced yield (9.53% wt) as well as antioxidant activity (IC_{50} = 95.4 $mg_{extract}/mL$) and total phenolic content of the extract (23.2 $mg_{GAE}/g_{extract}$). Thus, SFE could become a promising alternative to conventional extraction with ethanol, which exhibited the highest yield (28.5% wt) and a high antioxidant activity (IC_{50} = 3.2 $mg_{extract}/mL$), given SFE's shorter extraction duration.

Keywords: *Cistus creticus*; supercritical fluid extraction; process parameters; modeling; antioxidant activity

Check for updates

Academic Editors: Saša Savić, Sanja Petrovic and Zorica Knežević-Jugović

Received: 8 January 2026
Revised: 10 February 2026
Accepted: 24 February 2026
Published: 28 February 2026

Copyright: © 2026 by the authors. Licensee MDPI, Basel, Switzerland. This article is an open access article distributed under the terms and conditions of the Creative Commons Attribution (CC BY) license.

1. Introduction

Cistus (from the Greek word kistos) or Rock Rose belongs to the Cistaceae family and is a small and complex genus of dicotyledonous perennial herbaceous plants. This is due to the polymorphism of some cistus plants and the hybridization of related species [1]. The cistus plants have hard leaves and grow in open, stony, and infertile areas, found mostly in the Mediterranean region and on the Balearic and Canarian Islands [2]. Several of them are used as herbal tea infusions or extracts, particularly in folk medicine, due to their anti-inflammatory, antidiarrheal, skin protective, antibacterial and antifungal, antioxidant, antiviral, antiulcerogenic, wound healing, antimicrobial, cytotoxic, and anticancer activity [3–12]. Furthermore, the resin, ladano, from *Cistus creticus* (Crete and Cyprus) and

Cistus ladanifer (Spain), exported to many Arabic countries [10], contains a number of compounds (i.e., labdane triterpenes, terpenoids, etc.) with antioxidant, cytotoxic, antibacterial, antifungal, and anticancer properties [10,13–17]. It should be further noted that Cistus extracts, including that of *Cistus creticus*, have been tested for their cholinesterase inhibitory activity, leading to promising results for the prevention and treatment of neurodegenerative disorders such as Alzheimer's disease [18,19].

Nowadays, cistus essential oil is approved by the Food and Drugs Administration (FDA) as a food additive and flavoring agent [18], while a "Cistus tea" infusion from *C. creticus* leaves is already found in the markets as a dietary supplement to prevent chronic disease [20]. However, there is still a lack of exploitation for Cistus species [17].

The most common methods for recovering cistus oil include hydro- or steam-distillation [3,18], as well as a conventional solvent extraction using either a single solvent (water or organic solvents, such as ethyl acetate, ethanol, or methanol) or a mixture of solvents [12,21]. In some cases, successive extraction steps are also employed [22]. Lately, the use of deep eutectic solvents is also examined [23] as well as alternative extraction methods, namely ultrasound-assisted extraction, microwave-assisted extraction, and supercritical fluid extraction (SFE) [12,24–27]. However, the studies related to alternative extraction methods for Cistus species are still limited, particularly for SFE. Rincon et al. [26] examined the use of supercritical carbon dioxide (sCO_2) for the recovery of essential oil from *Cistus ladanifer* L. leaves, while Zhu et al. [27] studied the SFE of labdanum extract from branches and leaves of *Cistus ladaniferus* and compared it with that of hydrodistillation and Soxhlet extraction.

Supercritical fluid extraction, although still an expensive technique, is an interesting alternative, as carbon dioxide (CO_2), usually used as a supercritical solvent, is non-toxic, non-flammable, cheap, volatile, and readily available, with good dissolving power, which can be easily tuned by changing extraction temperature and pressure or using a co-solvent [28,29]. Furthermore, the extract is protected from being thermally or chemically degraded.

Thus, the aim of this work is the study of SFE of *Cistus creticus*, focusing on the effect of extraction pressure, temperature, and solvent flow rate on the extraction yield. To this purpose, a two-level full factorial design was employed, while the extraction kinetics were described using a mass transfer model proposed by Sovová [30,31]. This model assumes plug flow and takes into account the phase equilibrium and the diffusion-controlled regimes of the extraction process. Finally, for comparison, conventional techniques, such as hydrodistillation and Soxhlet extraction using ethanol and n-hexane as solvents, were also conducted.

2. Mathematical Model

In order to describe the kinetics of SFE of *C. creticus*, the mass balance model proposed by Sovová and co-workers [30,31] was employed. Actually, it is based on the extended Lack's plug flow model and assumes that the extraction comprises three stages, i.e., a fast stage (I) during which the easily accessible oil is extracted, a slow stage (III) where the trapped oil in the intact cells of plant material is extracted and an intermediate one (II), during which the transition from the fast to the slow stage occurs.

The equations of the model are the following:

$$e = \begin{cases} q\, y_r\, [1 - \exp(-Z)],\ q < q_m\ (I) \\ y_r\, [q - q_m exp(z_W - Z)],\ q_m < q < q_n\ (II) \\ x_0 - y_r/W\ ln\{1 + [exp(Wx_0/y_r) - 1]\, exp[W(q_m - q)]x_k/x_0\}, q \geq q_n (III) \end{cases} \quad (1)$$

where

$$q_m = (x_0 - x_k)/(y_r Z),\ q_n = q_m + \frac{1}{W} ln \left\{ \frac{\left[x_k + (x_0 - x_k) \exp\left(W \frac{x_0}{y_r} \right) \right]}{x_0} \right\} \quad (2)$$

$$\frac{z_w}{Z} = y_r/(W x_0) ln\{(x_0\ exp[W(q - q_m)] - x_k)/(x_0 - x_k)\} \quad (3)$$

$$Z = k_f a_o \rho / \left[\dot{q}(1 - \varepsilon)\rho_s \right] \text{and } W = k_s a_o / \left[\dot{q}(1 - \varepsilon) \right] \quad (4)$$

where q is the specific amount of solvent passed through the extractor (kg solvent/kg solute-free feed), y_r is the solubility of the solute in the solvent (kg solute/kg solvent), Z is the dimensionless mass transfer parameter in the fluid phase, q_m is the q value when extraction begins inside the particles, z_w is the dimensionless axial co-ordinate between fast and slow extraction, q_n is the q value when the easily accessible part of solute is all extracted, W is the dimensionless mass transfer parameter in the solid phase, x_0 is the initial total concentration of the solute in the solid (kg solute/kg solute-free feed), x_k is the concentration of the difficult accessible solute in the solid prior to the extraction (kg solute/kg solute-free feed), k_f is the solvent-phase mass transfer coefficient (m/s), and k_s is the solid-phase mass transfer coefficient (m/s).

The independent parameters of the model are: x_0, x_k, y_r, Z, and W. However, x_0 can be obtained experimentally by extraction till exhaustion of the extractable substances at the studied conditions, while the solute solubility (y_r), the so-called operational solubility, can be estimated from the initial slope of the extraction curve as shown in previous studies [32–34]. Consequently, the parameters finally fitted to the experimental data are: x_k, Z, and W.

3. Materials and Methods

3.1. Materials

Aerial parts of *Cistus creticus* subsp. *creticus*, including mainly leaves and flowers were collected in February 2020 in Crete island (at 35°23′36.0″ N and 24°53′02.0″ E), Greece, and were naturally dried. The raw material was stored in a dark place at ambient temperature, and its water content was found to be 7.49 ± 0.01 wt%, which is comparable to that reported in the literature [26]. Prior to each experiment, the *C. creticus* was ground with a commercial blender (Moulinex, Ecully, France) and sieved in a vertical vibratory sieve shaker. The mean particle diameter (d_p) was 250 μm.

The CO_2 (99.5 wt%) was purchased from Air-Liquide (Athens, Greece). Hexane (98.5% wt) and ethanol (96% *v*/*v*) were purchased from Carlo Erba Reagents (Val-de-Reuil, France). Ethyl acetate, orthophosphoric acid (analytical grade reagents), methanol (99.8%), and water (HPLC grade reagents) were acquired from Fisher Scientific International Inc. (Pittsburgh, PA, USA). Gallic acid (98%) (ACS reagents) was purchased from Acros Organics BVBA (Antwerp, Belgium). Free radical 2,2-diphenyl-1-picrylhydrazyl (DPPH) and Folin–Ciocalteu reagent were purchased from Sigma Aldrich Co. (Saint Louis, MO, USA) and Carlo Erba Reagents SAS (Milan, Italy), respectively.

3.2. Hydrodistillation

The *C. creticus* essential oil was obtained via hydrodistillation, using deionized water in a Clevenger-type apparatus. The solvent-to-feed ratio was set to 10:1, based on previous studies for other plant materials [34,35], and the duration was approximately 4 h. The hydrodistillation experiment was performed in triplicate.

3.3. Soxhlet Extraction

The grounded raw material was extracted using an organic solvent, i.e., hexane and ethanol, in a Soxhlet extraction apparatus. A typical solvent to feed ratio of 20:1 was employed based on previous studies, and the extraction was stopped once the recovered extract became colorless, after approx. 6 h. The solvent was removed from the extract under vacuum using a rotary evaporator (Hei-VAP Advantage ML, Heidolph Instruments GmbH and Co. KG, Bayern, Germany). All experiments were conducted in triplicate.

3.4. Supercritical Fluid Extraction (SFE)

The SFE experiments were conducted in a bench-scale apparatus (SFE-500, SEPAREX CHIMIE FINE, Champigneulles, France). A detailed description of the SFE apparatus and the experimental procedure is presented in a previous publication [36].

In this study, a quantity of approximately 50 g of ground material was placed in the extractor vessel along with two layers of glass beads (d = 4.5 mm) at the top and the bottom of the vessel in order to reduce its dead space and enable the uniform distribution of the solvent flow. The operating conditions of the two separators were 80 bar and 15 bar, respectively, at a temperature equal to 8 °C. The extraction conditions examined, namely extraction pressure and temperature, and solvent flow rate, are reported in Table 1, as a result of a two-level factorial design with a central point, while the experimental error was determined through a quadruplicate repetition of the central point. Based on previous studies, the particle size of the raw material (approx. 250 μm) was sufficiently small to enhance solvent accessibility to the oil due to cell disruption, while being large enough to minimize losses associated with the comminution process [26,28]. The extraction yield (kg extract/kg feed) was determined gravimetrically based on the weight loss of the extraction vessel at the end of the extraction (150 min), while for the kinetic study, experiments were interrupted at regular intervals to measure weight loss.

Table 1. SFE operating conditions based on the two-level factorial design.

Experiment	T (°C)	P (Bar)	CO_2 Flow Rate (kg/h)	CO_2 Density [1] (kg/lt)
SFE-1	40	110	1	0.684
SFE-2	40	250	1	0.879
SFE-3	60	110	1	0.358
SFE-4	60	250	1	0.787
SFE-5	40	110	3	0.684
SFE-6	40	250	3	0.879
SFE-7	60	110	3	0.358
SFE-8	60	250	3	0.787
SFE-9	50	180	2	0.757
SFE-10	50	180	2	0.757
SFE-11	50	180	2	0.757
SFE-12	50	180	2	0.757

[1] Density data were taken from NIST [37].

Finally, the effect of a co-solvent addition was examined at 250 bar, 60 °C, and 3 kg/h. To this purpose, a piston pump was employed for the addition of ethanol (EtOH) as co-solvent in a concentration equal to 5% wt. This experiment was conducted in duplicate.

3.5. Extract Analysis

3.5.1. GC–MS Analysis

GC–MS analysis was carried out on an HP 6890 gas chromatograph (Hewlett-Packard, Palo Alto, CA, USA) equipped with a HP 5973 selective mass detector (Hewlett-Packard,

Palo Alto, CA, USA) in EI ionization mode (70 eV) and a capillary column HP-5 MS (Hewlett-Packard, Palo Alto, CA, USA) (30 m × 0.32 mm; film thickness, 0.25 μm). Helium was the carrier gas, at a flow rate of 0.8 mL/min. The injection temperature was set to 220 °C, while the column temperature was initially kept at 60 °C for 5 min and then gradually increased to 280 °C with a rate of 3 °C/min, which was maintained for 15 min. For the components identification, their mass spectra were compared to those reported in the libraries of Wiley 275 and NIST.

3.5.2. Spectrophotometric Assays

The extracts' antioxidant activity was determined via the 2,2-diphenyl-1-picrylhydrazyl (*DPPH*) free radical scavenging assay in terms of the half-maximal inhibitory concentration (IC_{50}). The IC_{50} was detected at 515 nm and expressed as the extract concentration (mg_{extr}/mL). According to the assay procedure, 3.9 mL of *DDPH* was mixed with 0.1 mL of extract solution, the mixture was vortexed, and after 20 min of incubation, the absorbance at 515 nm was measured. Thus, the DPPH ($\%DPPH_{REM}$) was calculated as follows:

$$\%DPPH_{REM} = \frac{[DPPH]_t}{[DPPH]_{t=0}} * 100 \quad (5)$$

where $[DPPH]_t$ is the absorbance at 515 nm after 20 min, and $[DPPH]_{t=0}$ is the initial absorbance of the *DPPH* solution. The IC_{50} value was then determined via the plot of the percentage of *DPPH* remaining against the concentration of the extract.

Total phenolic content (TPC) was also measured through the Folin–Ciocalteu assay, as described by Drosou et al. [38]. TPC was detected at 765 nm and expressed in terms of mg of gallic acid equivalent per gram of extract (mg_{GAE}/g_{extr}).

All measurements were conducted in triplicate.

3.6. Experimental Design and Statistical Analysis

A two-level factorial design was employed for the experimental design. Specifically, the effect of three parameters (factors), namely extraction pressure, temperature, and solvent flow rate, at two levels and a center point (4 repetitions) was examined, while the extraction yield at a fixed extraction time equal to 150 min was employed as a response. The parameters range was: 110–250 bar for pressure, 40–60 °C for temperature and 1–3 kg/h for the solvent flow rate.

The experimental data were subjected to analysis of variance (ANOVA) using Design Expert v13 software, trial version (Stat-Ease Inc., Minneapolis, MN, USA). The equation applied was a linear function of the examined factors and their interactions, as shown by the equation below:

$$Yield\ (\%wt) = a_0 + a_1 \times T + a_2 \times P + a_3 \times F + a_4 \times T \times P + a_5 \times T \times F + a_6 \times P \times F + a_7 \times T \times P \times F \quad (6)$$

where T is the extraction temperature, P the extraction pressure, F the solvent flow rate, and α_i (i = 0–7) the fitted parameters, corresponding to the constant, linear and two-factor interaction coefficients.

4. Results and Discussion

4.1. Hydrodistillation

The essential oil content of *C. creticus* was (0.040 ± 0.002)% wt as determined by the hydrodistillation process. According to previous studies, the essential oil content of *C. creticus* was found to range from 0.01 to 0.6% wt, as it depends on various factors, e.g., the part of the plant (flowers, leaves, etc), the harvesting year and season, origin, etc. [18,39–41].

4.2. Soxhlet Extraction

The conventional Soxhlet extraction of *C. creticus* with a non-polar (n-hexane) and a polar solvent (ethanol) led to a yield equal to (4.6 ± 0.3)% wt and (28.5 ± 1.1)% wt respectively. As expected, ethanol, due to its higher polarity, leads to a higher extraction yield, in contrast to the less polar hexane, which extracts compounds of low or no polarity. The yields of this study are in accordance with those reported in the literature for *C. creticus* or other species of cistus [22,42], taking into account the differences in the raw material due to harvesting year/season, species, region, etc.

4.3. Supercritical Fluid Extraction (SFE)

The SFE yield results are reported in Table 2, while the effect of the examined process parameters (pressure, temperature, and solvent flow rate) is also presented graphically in Figures 1 and 2, in which the extraction yield is depicted as a function of the specific amount of CO_2 consumed.

Table 2. Yields (% wt) obtained by SFE of *C. creticus* at an extraction time of 150 min.

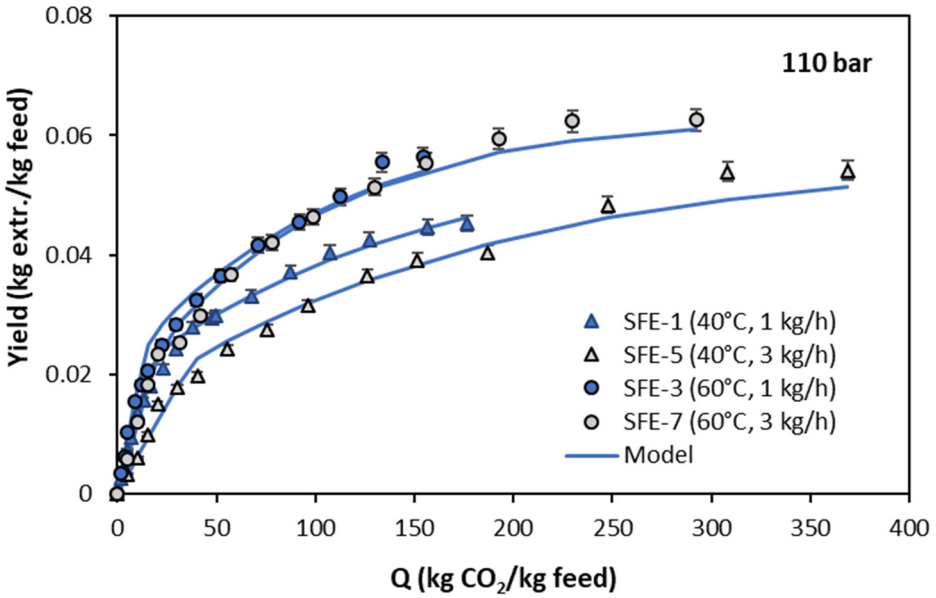
Experiment	Yield (% wt)
SFE-1	2.99
SFE-2	5.86
SFE-3	3.65
SFE-4	6.85
SFE-5	3.90
SFE-6	6.44
SFE-7	5.54
SFE-8	8.58
SFE-9	5.31
SFE-10	5.18
SFE-11	5.20
SFE-12	5.64

Depending on the extraction conditions, the yield obtained after 150 min of extraction varied from approx. 3 to 8.6%wt, while the experimental error based on the center point experiments was found equal to ±2.9%. Due to a lack of data for SFE of *C. creticus*, the yields of this work were compared with those of Zhu et al. [27] and Rincon et al. [26] regarding SFE of *Cistus ladanifer* L. Thus, Zhu et al. [27] reported a yield equal to 6.6% at 280 bar, 40 °C, and 30 L/h, which is comparable to the yields of this work, taking into account the differences regarding the raw material and the extraction conditions. In the case of Rincon et al. [26], the yields are significantly smaller, mainly due to the fact that their study targeted the extraction of cistus essential oil at lower extraction pressures solely.

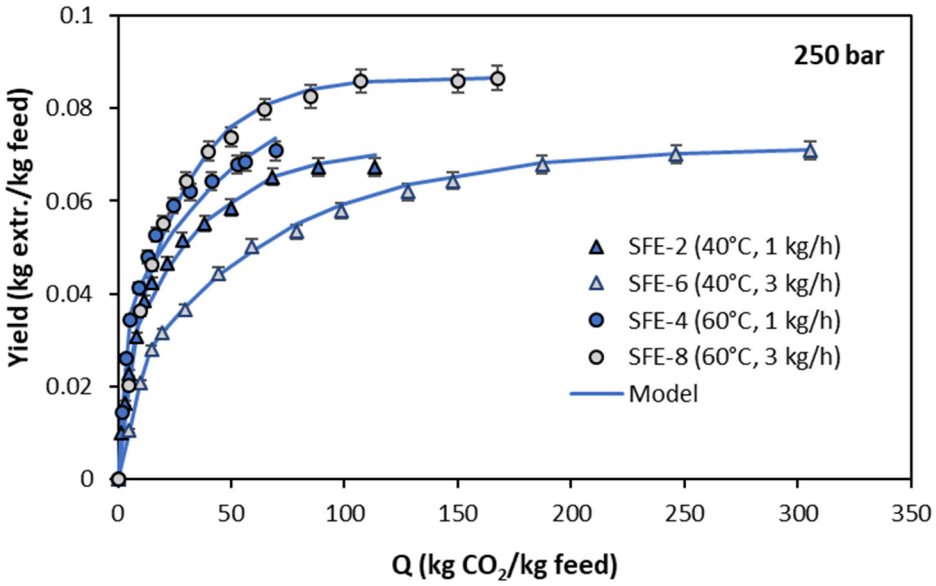
Concerning the impact of process parameters, it is shown that the pressure increase has a positive effect on yield due to the increase in the CO_2 density (Table 1) and consequently its dissolving ability (Figure 1). Similarly, at constant pressure, the temperature increase leads to higher yields (Figure 2), as the increase in solute vapor pressure dominates over the decrease in CO_2 density with temperature.

As for the flow rate, it is shown that the extraction rate is increased with increasing flow rate, but at the expense of the CO_2 consumption. That is why, at a fixed extraction time, the increase in flow rate leads to a higher yield (Table 2). This is in agreement with the findings of other researchers [43]. It should also be noted that initially, during the first stage of the extraction, the slope of the linear part of the extraction curve becomes smaller as the flow rate increases. This is more pronounced at 250 bar in Figure 1, and can be attributed to the fact that at a lower flow rate, the solvent remains in the extractor for a longer period

of time, reaching this way closer to its saturation point, i.e., closer to the solubility value, which governs this extraction stage.



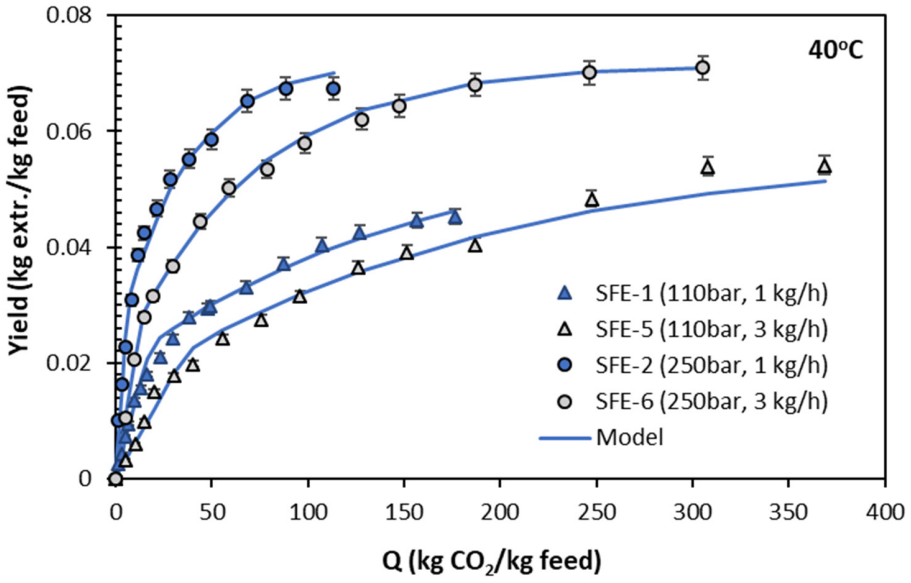
(**a**)



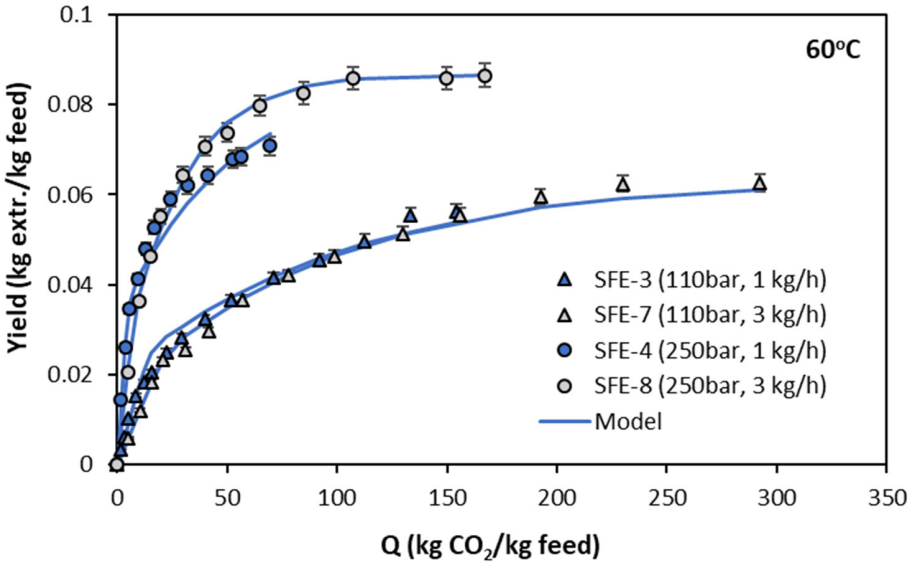
(**b**)

Figure 1. Effect of temperature and flow rate on the extraction yield versus the specific amount of solvent (Q) at pressure: (**a**) 110 bar and (**b**) 250 bar. Modeling results are also presented. The error bars stand for the experimental error.

Overall, the pressure effect is proven to be the dominant one regarding the yield of the process, which is in accordance with the findings of the statistical analysis presented in the next section.



(**a**)



(**b**)

Figure 2. Effect of pressure and flow rate on the extraction yield versus the specific amount of solvent (Q) at constant temperature: (**a**) 40 °C and (**b**) 60 °C. Modeling results are also presented. The error bars stand for the experimental error.

4.4. Statistical Analysis

Statistical analysis (ANOVA) of the experimental data was performed, and the corresponding results are presented in Table 3. Specifically, the F-tests' *p*-values for all three individual factors, i.e., pressure, temperature, and flow rate, and the combined factor of temperature and flow rate, are lower than 0.05, indicating that they are significant model terms. Actually, their influence accounts for more than 98% of the total effect on the response, confirming their significance. However, the pressure effect is the dominant one, as its contribution to the effect on the yield response is higher than 68%.

Based on the above analysis, Equation (6) becomes simpler as non-significant terms were omitted:

$$Yield\ (\%\ \mathrm{wt}) = -0.32976 + 0.020786 \times P + 0.01475 \times T - 0.6850 \times F + 0.0265 \times T \times F \quad (7)$$

The developed model is proven to be significant ($p < 0.0001$), while the lack of fit is insignificant ($p > 0.1$). The coefficient of determination (R^2) acquires a high value (approx. 0.99), while the adjusted R^2 is only slightly lower (0.98). Furthermore, the predicted R^2 is equal to 0.96 and thus in reasonable agreement with the adjusted one, as their difference is smaller than 0.2. The model accuracy is also depicted in Figure 3, where the predicted yield values versus the experimental ones are presented. Actually, the absolute average relative deviation ($AAD\% = \frac{1}{NP}\sum_1^{NP} \frac{abs\left(Yield_{exp} - Yield_{calc}\right)}{Yield_{exp}} * 100$, NP: number of data) of the model is 2.8%. Finally, the coefficient of variation (C.V.%) is found to be 3.91%, indicating the accurate yield prediction as well.

Table 3. The results of ANOVA for the reduced 2 FI (two Factor Interaction) model.

Source	% Contribution	*p*-Value	
Model		<0.0001	*significant*
P	68.4	<0.0001	*significant*
T	14.8	<0.0001	*significant*
F	13.2	<0.0001	*significant*
T·F	2.3	0.00959	*significant*
Lack of Fit		0.524	*not significant*
R^2	0.9873	**Predicted R^2**	0.9586
Adjusted R^2	0.9799	**C.V.%**	3.91

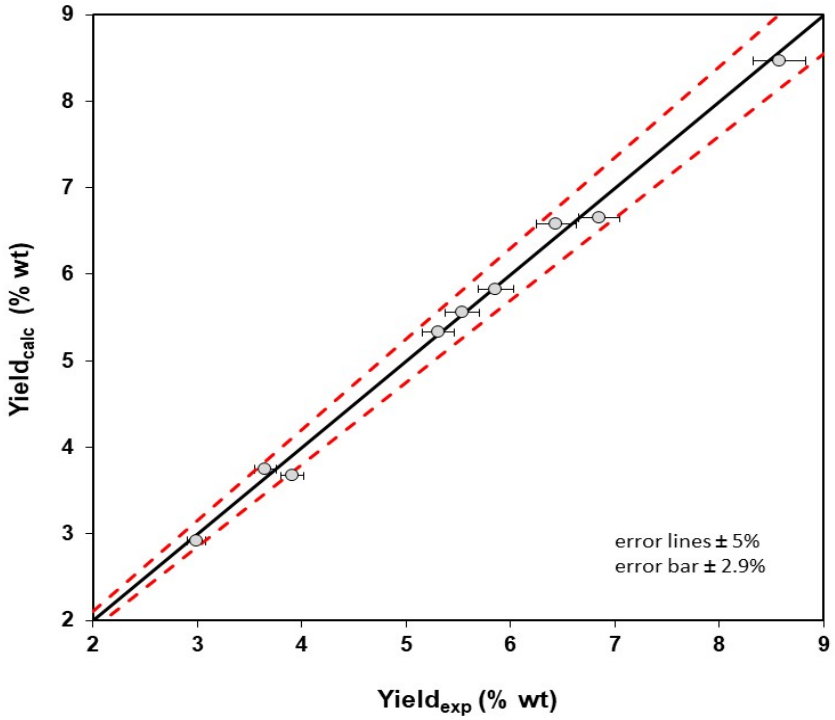


Figure 3. Predicted yield (%wt) by Equation (7) versus the experimental one. The error bars stand for the experimental error and the red dashed lines for the error lines.

The effects of the examined parameters are also depicted in surface plots of the developed model (Figure 4), highlighting the positive effect of all three parameters on yield. Consequently, the highest yield was estimated at 250 bar, 60 °C, and 3 kg/h. Moreover, the dominant effect of pressure is confirmed.

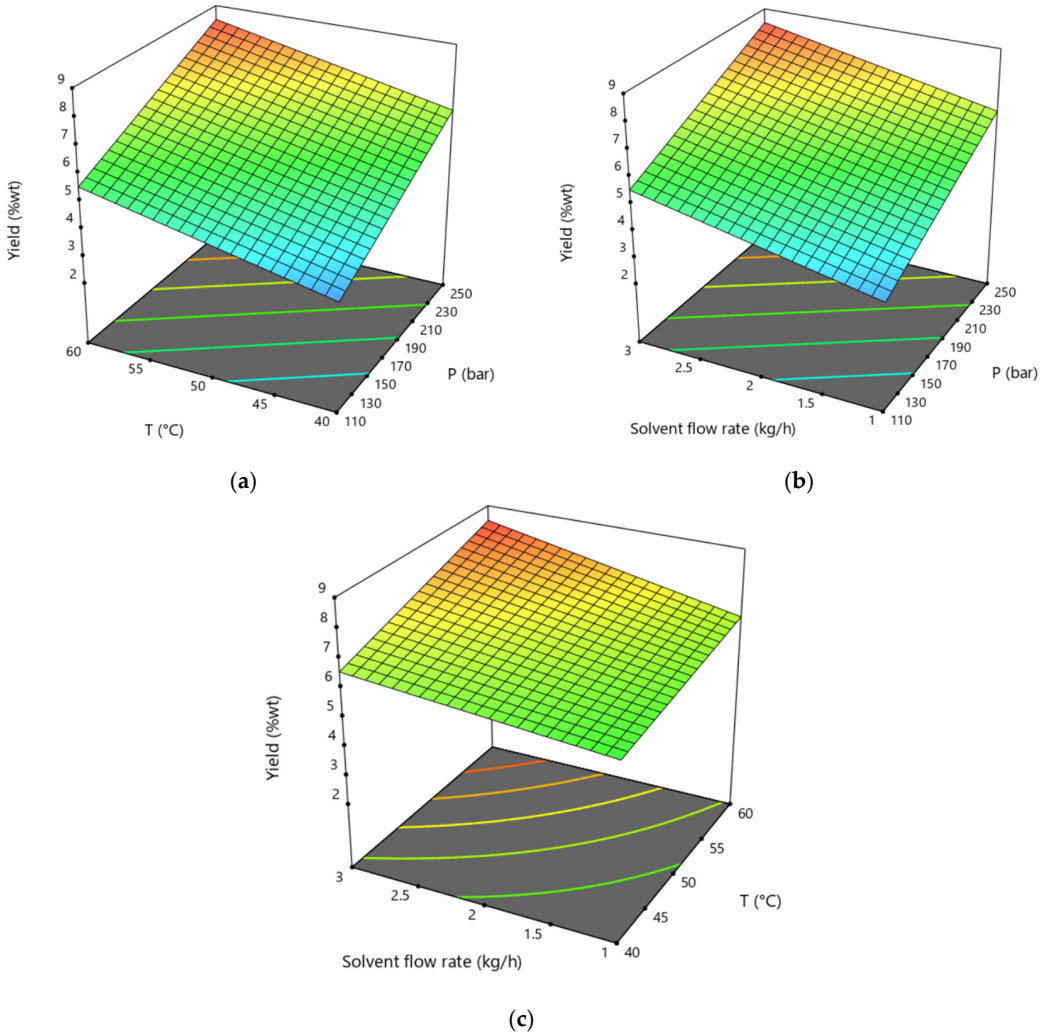


Figure 4. 3-D surface plots presenting the effect of pressure, temperature, and solvent flow rate on yield: (**a**) pressure-temperature effect at a solvent flow rate of 3 kg/h, (**b**) pressure-flow rate effect at 60 °C, and (**c**) temperature-solvent flow rate at 250 bar.

4.5. Modeling of SFE Curves

The experimental results were satisfactorily described by the Sovová model as shown in Table 4 along with the determined model parameters, and Figures 1 and 2.

Table 4. Estimated parameters of the Sovová model regarding the SFE of *C. creticus*.

Experiment	y_r	x_0	x_k	$Z \times \dot{q}$ 10^2 (s^{-1})	$W \times \dot{q}$ 10^4 (s^{-1})	AAD% [1]
SFE-1	0.00144	0.060	0.0366	1.670	0.427	5.04
SFE-2	0.00510	0.077	0.0470	2.243	1.788	4.00
SFE-3	0.00191	0.067	0.0409	1.734	0.625	5.64
SFE-4	0.00770	0.095	0.0580	1.841	1.324	5.16
SFE-5	0.00144	0.060	0.0366	0.962	0.991	5.64
SFE-6	0.00510	0.077	0.0470	0.928	2.532	1.29
SFE-7	0.00191	0.067	0.0409	1.729	2.029	2.87
SFE-8	0.00770	0.095	0.0580	1.396	6.776	1.55
SFE-9	0.00180	0.071	0.0433	2.299	2.286	5.24

[1] $AAD\% = \frac{1}{NP}\sum_1^{NP} \frac{abs(e_{exp} - e_{calc})}{e_{exp}} * 100$; NP: number of data points.

More specifically, the values of x_0 were determined experimentally by extraction till exhaustion of the extractable substances at the studied conditions. That is why extraction

curves are extended to extraction times higher than 150 min. Thus, it was demonstrated that x_0 depends on pressure and temperature, a finding that has also been reported by other authors [33,43]. As for y_r, it was considered constant at different flow rates and set equal to the initial slope of the curve resulting from the lower flow rate at a certain pressure and temperature. This is justified by the fact that the longer residence of CO_2 in the extractor at a lower flow rate allows y_r to acquire values closer to the real solubility. It is also observed that both x_0 and y_r increase with increasing temperature and pressure, in the same manner that yield is affected by them, as previously discussed.

In the case of x_k, it was shown that it is affected by the value of x_0. However, the grinding efficiency $r = \frac{x_0 - x_k}{x_0}$ was found to be constant and equal to 0.39 in all cases examined, since the mean particle diameter of the raw material was the same for all experiments.

Regarding the mass transfer parameters, they acquire reasonable values comparable to those found in the literature [31,34,44,45], taking into account that they are referred to different natural matrices. Actually, the solvent phase mass transfer parameter ($Z \times \dot{q}$) decreases with increasing flow rate, showing that the solvent residence time and solubility play a key role in the first fast part of the extraction curve. Also, its values are two orders of magnitude higher than those of ($W \times \dot{q}$), which is typical due to the decrease in extraction rate in the third slow stage of extraction [34].

In the case of ($W \times \dot{q}$), it is observed that it increases with the increase of flow rate, showing that the external mass transfer affects the third extraction period, in which the intraparticle mass transfer is assumed to be the dominant one. This phenomenon has also been observed by other researchers [34,45,46]. As for the other operational parameters, i.e., pressure and temperature, they also affect ($W \times \dot{q}$), but no safe conclusions can be obtained due to the variation in xo.

4.6. Comparison of SFE with Conventional Extraction Methods

4.6.1. SFE and Hydrodistillation

In terms of extraction yield, the hydrodistillation yield (0.04% wt) was, as expected, the lowest one since it refers solely to the recovery of the essential oil. Thus, the SFE yields were much higher (approx. 3 to 8.6%) at all conditions examined due to the co-extraction of other compounds as well.

This was also verified by the GC–MS analysis of the extracts obtained by hydrodistillation and SFE at intermediate conditions, i.e., 180 bar, 50 °C, and 2 kg/h. Actually, the corresponding chromatograms are presented in Figures 5 and 6, while the main compounds identified are presented in Table 5. It is evident that the SFE extract contains heavier compounds, like the long-chain aliphatic hydrocarbons 9-nonadecene and 17-pentatriacontene, as essential oil is co-extracted with waxy compounds at 180 bar and 50 °C. The identified compounds have been reported by other researchers as well [18,47]. However, since the oil composition is highly affected by cistus species, the part of the plant extracted, the origin, the harvest year/season, etc., a direct comparison is not possible.

The main compounds of hydrodistillation (HD) extract were found to be carvacrol, a phenolic monoterpene, known for its antioxidant, anti-inflammatory, anti-microbial, etc. activities [48], hexadecanoic acid (i.e., palmitic acid), and linoleic acid. Both these fatty acids were reported to exhibit cytotoxic activity [49], while linoleic acid, as an omega-6 fatty acid, is known for its beneficial properties to human health and skin (anti-inflammatory, acne reduction, emollient, antioxidant), and hence it is very popular in the cosmetic industry [50]. In the case of SFE extract, the most abundant compounds identified were the fatty acids, hexadecanoic and linoleic acid, and the long-chain hydrocarbons, 9-nonadecene and 17-pentatriacontene. Specifically, linoleic acid content in the SFE extract is higher than that reported for the HD extract. Also, the presence of long-chain hydrocarbons in plant extracts,

like 17-pentatriacontene, contributes to their anti-inflammatory, anticancer, antibacterial, antimicrobial, and antiarthritic properties [51,52]. Finally, labdane-type diterpenes, i.e., manoyl oxide and 13-epi-manoyl oxide, were also detected in both extracts. These diterpenes exhibit anti-inflammatory, antimicrobial, antinociceptive, and sedative activities, justifying the use of cistus species in folk medicine [15,16,48].

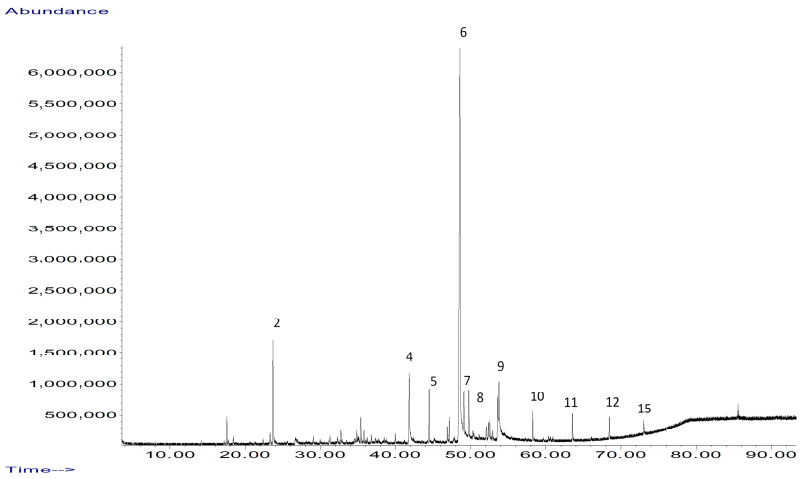


Figure 5. GC chromatogram for hydrodistillation extract of *C. creticus* (for peak identification see Table 5).

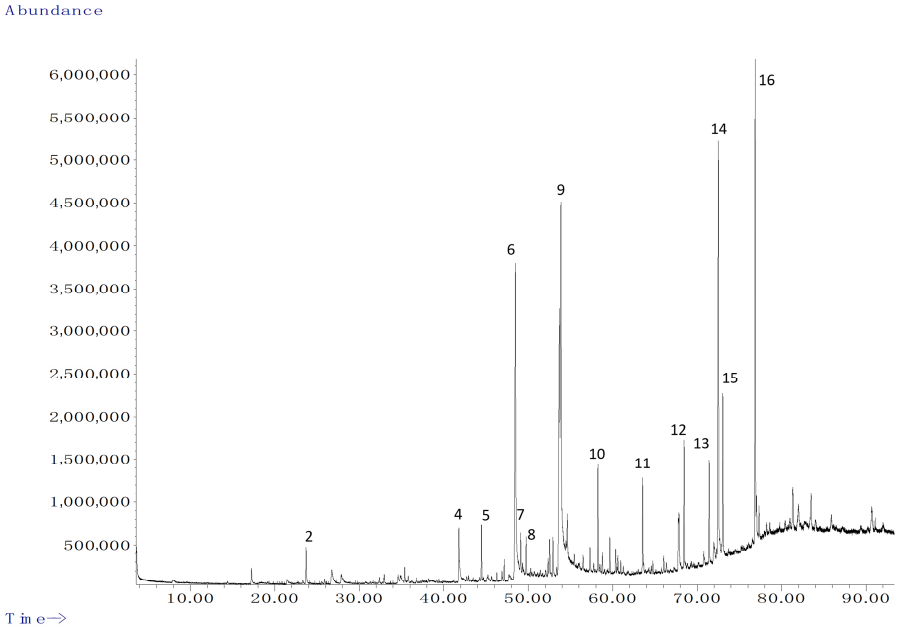


Figure 6. GC chromatogram for SFE-9 extract of *C. creticus* (for peak identification see Table 5).

Table 5. Main compounds identified by GC–MS analysis of *C. creticus* essential oil obtained by hydrodistillation (HD) and SFE extract (SFE-9), and their composition (% of total peak area).

No	Main Compounds	Area %	
		HD	SFE-9
1	Thymol	0.92	0.2
2	Carvacrol	7.56	1.05
3	Viridiflorol	1.71	0.37
4	Tetradecanoic acid	4.96	1.80
5	2-pentadecanone,6,10,14-trimethyl	3.27	1.29

Table 5. *Cont.*

No	Main Compounds	Area %	
		HD	SFE-9
6	Hexadecanoic acid	46.9	8.5
7	Manoyl oxide	3.09	1.08
8	13-epi-manoyl oxide	3.34	1.00
9	Linoleic acid	9.88	24.43
10	Tricosane	1.86	2.65
11	Pentacosane	2.23	2.44
12	Heptacosane	2.42	3.32
13	Squalene	0.02	2.69
14	9-Nonadecene	0.02	13.00
15	Triacontane	1.19	4.08
16	17-Pentatriacontene	0.012	13.36

4.6.2. SFE and Soxhlet Extraction

The comparison between SFE and Soxhlet extraction showed that Soxhlet extraction with ethanol led to the highest yield (28.5% wt), followed by SFE at high temperature and pressure with a yield equal to 8.58% wt, while the hexane extraction resulted in a yield of 4.6%wt. However, the main disadvantage of the conventional extraction methods is the prolonged duration of the process.

The extracts were subjected to a DPPH assay to determine their antioxidant activity, expressed as IC_{50} values. However, most of the extracts did not exhibit significant antioxidant activity via this assay, despite the presence of bioactive compounds identified previously by GC–MS analysis, possibly due to antagonistic effects among the constituents or the presence of other non-bioactive compounds [53,54]. Thus, focus was given to the best extracts in terms of bioactivity and yield, for which total phenolic content (TPC) was also measured. The results are presented in Table 6, where it is shown that the ethanolic extract exhibits high antioxidant activity comparable to that of ascorbic acid. On the other hand, the SFE extract does not demonstrate significant activity according to the DPPH assay. However, the addition of only a small amount of co-solvent to sCO_2, i.e., 5% wt ethanol, significantly improved antioxidant activity and TPC, due to the increase in the solvent's polarity, as well as the yield (Table 2).

Table 6. Antioxidant activity (IC_{50}) and total phenolic content (TPC) for *C. creticus* extracts.

Extract	IC_{50} ($mg_{extract}/mL$)	TPC ($mg_{GAE}/g_{extract}$)
EtOH	3.2 ± 0.2	171.7 ± 16.8
SFE-8	-	14.5 ± 1.5
SFE with 5% EtOH (250 bar, 60 °C, 3 kg/h)	95.4 ± 4.8	23.2 ± 2.5
Ascorbic acid	2.1 ± 0.1	-

5. Conclusions

In this work, the SFE of *C. creticus* was examined, giving emphasis on the effect of pressure, temperature, and solvent flow rate on the extraction yield, by employing a two-level factorial design for the experiments. Thus, it was shown that the extraction yield was enhanced by temperature and, particularly, by pressure increase. As for the solvent flow rate, its increase affected the extraction rate positively. Consequently, the maximum extraction yield (8.58% wt) was obtained at 250 bar, 60 °C, and 3 kg/h.

The aforementioned effects were verified by the analysis of variance of the experimental data (ANOVA). Furthermore, a mathematical model was developed to describe yield as a function of the process parameters, demonstrating good agreement between predicted and experimental yields. Additionally, the extraction curves were simulated successfully by the mass balance model of Sovová, proving that it can be a useful tool for the scale-up and optimization of the process.

Furthermore, a comparison between extracts obtained by conventional hydrodistillation and SFE was conducted. As expected, given the extraction pressures examined, SFE resulted in higher extraction yields than hydrodistillation, promoting the co-extraction of heavier compounds as confirmed by the GC–MS analysis. The main compound identified in the HD extract was hexadecanoic acid (46.9%), whereas in the SFE-9 extract it was linoleic acid (24.4%). However, no significant antioxidant activity was determined in terms of IC_{50}. Finally, the comparison of SFE with Soxhlet extraction showed that the use of a polar solvent, namely ethanol, in Soxhlet led to high extraction yield (28.5% wt) and antioxidant activity of the extract, in contrast to Soxhlet extraction with hexane and SFE. Nevertheless, it was demonstrated that the addition of a small amount of co-solvent can significantly enhance the efficiency of SFE in terms of yield, antioxidant activity (IC_{50}), and TPC, which, combined with the shorter process duration, can render SFE an attractive alternative.

Supplementary Materials: The following supporting information can be downloaded at: https://www.mdpi.com/article/10.3390/separations13030079/s1, Table S1. Compounds identified via GC-MS analysis of C. creticus essential oil obtained by hydro-distillation (HD) and SFE extract (SFE-9), and their composition (% of total peak area).

Author Contributions: Conceptualization, K.M.; methodology, M.C. and V.L.; software, M.C. and V.L.; validation, M.C. and V.L. and K.M.; investigation, M.C. and V.L.; data curation, M.C. and V.L. and K.M.; writing—original draft preparation, V.L.; writing—review and editing, V.L. and K.M.; supervision, K.M. All authors have read and agreed to the published version of the manuscript.

Funding: This research received no external funding.

Data Availability Statement: The original contributions presented in this study are included in the article/Supplementary Material. Further inquiries can be directed to the corresponding author.

Acknowledgments: The authors kindly acknowledge APIVITA SA for the supply of raw material, the Food Chemistry Technology Laboratory, and the Design Process Analysis Laboratory of NTUA for contributing to the analysis of the extracts.

Conflicts of Interest: The authors declare no conflicts of interest.

References

1. Ellul, P.; Boscaiu, M.; Vicente, O.; Moreno, V.; Rosello, J.A. Intra and interspecific variation in DNA content in *Cistus* (*Cistaceae*). *Ann. Bot.* **2002**, *90*, 345–351. [CrossRef]
2. Guzman, B.; Vargas, P. Systematics, character evolution, and biogeography of *Cistus* L. (*Cistaceae*) based on ITS, trnL-trnF, and matK sequences. *Mol. Phylogenet. Evol.* **2005**, *37*, 644–660. [CrossRef] [PubMed]
3. Barrajón-Catalán, E.; Fernández-Arroyo, S.; Roldán, C.; Guillén, E.; Saura, D.; Segura-Carretero, A.; Micol, V. A systematic study of the polyphenolic composition of aqueous extracts deriving from several *Cistus* genus species: Evolutionary relationship. *Phytochem. Anal.* **2011**, *22*, 303–312. [CrossRef] [PubMed]
4. Morales-Soto, A.; Oruna-Concha, M.J.; Elmore, J.S.; Barrajon-Catalan, E.; Micol, V.; Roldan, C.; Segura-Carretero, A. Volatile profile of Spanish *Cistus* plants as sources of antimicrobials for industrial application. *Ind. Crops Prod.* **2015**, *74*, 425–433. [CrossRef]
5. Demetzos, C.; Mitaku, S.; Loukis, A.; Harvala, C.; Gaily, A. A new drimane sesquiterpene, isomers of manoyloxide and other volatile constituents from the resin "Ladano" of *Cistus incanus* subsp. *creticus* (L.) *Heywood*. *J. Essent. Oil Res.* **1994**, *6*, 37–41. [CrossRef]
6. Petereit, F.; Kolodziej, H.; Nahrstedt, A. Flavan-3-ols and proanthocyanidins from *Cistus incanus*. *Phytochemistry* **1991**, *30*, 981–985. [CrossRef]

7. Danne, A.; Petereit, F.; Nahrstedt, A. Proanthocyanidins from *Cistus incanus*. *Phytochemistry* **1993**, *34*, 1129–1133. [CrossRef]
8. Attaguile, G.; Russo, A.; Campisi, A.; Savoca, F.; Acquaviva, R.; Ragusa, N.; Vanella, A. Antioxidant activity and protective effect on DNA cleavage of extracts from *Cistus incanus* L. and *Cistus monspeliensis* L. *Cell Biol. Toxicol.* **2000**, *16*, 83–90. [CrossRef]
9. Barrajón-Catalán, E.; Tomás-Menor, L.; Morales-Soto, A.; Bruñá, N.M.; López, D.S.; Segura-Carretero, A.; Micol, V. Rockroses (*Cistus* sp.) Oils. In *Essential Oils in Food Preservation, Flavor and Safety*; Preedy, V.R., Ed.; Academic Press (Elsevier): San Diego, CA, USA, 2016; Volume 74, pp. 649–656.
10. Papaefthimiou, D.; Papanikolaou, A.; Falara, V.; Givanoudi, S.; Kostas, S.; Kanellis, A.K. Genus *Cistus*: A model for exploring labdane-type diterpenes' biosynthesis and a natural source of high value products with biological, aromatic, and pharmacological properties. *Front. Chem.* **2014**, *2*, 35. [CrossRef] [PubMed]
11. Zalegh, I.; Akssira, M.; Bourhia, M.; Mellouki, F.; Rhallabi, N.; Salamatullah, A.M.; Alkaltham, M.S.; Alyahya, H.K.; Mhand, R.A. A Review on *Cistus* sp.: Phytochemical and Antimicrobial Activities. *Plants* **2021**, *10*, 1214. [CrossRef]
12. Rivas, M.A. An overview of the antifungal potential for aromatic plant extracts in agriculture and the food industry: A comprehensive analysis focusing on the *Rubus*, *Cistus* and *Quercus* genera against fungal infections of crops and food. *Int. J. Food Microbiol.* **2025**, *436*, 111209. [CrossRef]
13. Kuchta, K.; Tung, N.H.; Ohta, T.; Uto, T.; Raekiansyah, M.; Grötzinger, K.; Rausch, H.; Shoyama, Y.; Rauwald, H.W.; Morita, K. The old pharmaceutical oleoresin labdanum of *Cistus creticus* L. exerts pronounced in vitro anti-dengue virus activity. *J. Ethnopharmacol.* **2020**, *257*, 112316. [CrossRef]
14. Rauwald, H.W.; Liebold, T.; Grötzinger, K.; Lehmann, J.; Kuchta, K. Labdanum and Labdanes of *Cistus creticus* and *C. ladanifer*: Anti-Borrelia activity and its phytochemical profiling. *Phytomedicine* **2019**, *60*, 152977. [CrossRef]
15. Chinou, I.; Demetzos, C.; Harvala, C.; Roussakis, C.; Verbist, J.F. Cytotoxic and antibacterial labdane-type diterpenes from the aerial parts of *Cistus incanus* subsp. *creticus*. *Planta Med.* **1994**, *60*, 34–36. [CrossRef] [PubMed]
16. Demetzos, C.; Mitaku, S.; Couladis, M.; Harvala, C.; Kokkinopoulos, D. Natural metabolites of ent-13-epi-manoyloxide and other cytotoxic diterpenes from the resin "LADANO" of *Cistus creticus*. *Planta Med.* **1994**, *60*, 590–591. [CrossRef] [PubMed]
17. Alves-Ferreira, J.; Duarte, L.C.; Fernandes, M.C.; Pereira, H.; Carvalheiro, F. *Cistus ladanifer* as a Potential Feedstock for Biorefineries: A Review. *Energies* **2023**, *16*, 391. [CrossRef]
18. Loizzo, M.R.; Jemia, M.B.; Senatore, F.; Bruno, M.; Menichini, F.; Tundis, R. Chemistry and functional properties in prevention of neurodegenerative disorders of five *Cistus* species essential oils. *Food Chem. Toxicol.* **2013**, *59*, 586–594. [CrossRef]
19. Kahraman, Ç.; Gönülalan, E.M.; Koçak, E.; Şen Gökmen, F.; Gündüz, M.G.; Nemutlu, E.; Tatli Çankaya, İ.İ. Non-targeted metabolomic profiling of *Cistus* species and association with anticholinesterase efficacy for Alzheimer's disease: In vitro and in silico evaluation. *J. Ethnopharmacol.* **2026**, *355*, 120692. [CrossRef] [PubMed]
20. Riehle, P.; Vollmer, M.; Rohn, S. Phenolic compounds in *Cistus incanus* herbal infusions—Antioxidant capacity and thermal stability during the brewing process. *Food Res. Int.* **2013**, *53*, 891–899. [CrossRef]
21. Pekacar, S.; Ozüpek, B.; Akkol, E.K.; Tastan, H.; Ersan, H.; Orhan, D.D. Identification of bioactive components on antihemorrhoidal activity of *Cistus laurifolius* L. using RP-HPLC and LC-QTOF-MS. *J. Ethnopharmacol.* **2024**, *319*, 117122. [CrossRef]
22. Palaiogiannis, D.; Chatzimitakos, T.; Athanasiadis, V.; Bozinou, E.; Makris, D.P.; Lalas, S.I. Successive Solvent Extraction of Polyphenols and Flavonoids from *Cistus creticus* L. Leaves. *Oxygen* **2023**, *3*, 274–286. [CrossRef]
23. Palaiogiannis, D.; Athanasiadis, V.; Bozinou, E.; Chatzimitakos, T.; Makris, D.P.; Lalas, S.I. Extraction of polyphenolic and volatile compounds from *Cistus creticus* using deep eutectic solvents and pulsed electric fields. *Compounds* **2022**, *2*, 311–320. [CrossRef]
24. Christou, A.; Nikola, F.; Goulas, V. Optimization of the Ultrasound-Assisted Extraction of Phenolic Antioxidants from *Cistus salvifolius* L. Using Response Surface Methodology. *Chem. Biodivers.* **2025**, *22*, e202401337. [CrossRef]
25. El Hachlafi, N.; Kandsi, F.; Elbouzidi, A.; Lafdil, F.Z.; Nouioura, G.; Abdallah, E.M.; Abdnim, R.; Bnouham, M.; Al-Mijalli, S.H.; Mrabti, H.N.; et al. Extraction of Bioactive Compound-Rich Essential Oil from *Cistus ladanifer* L. by Microwave-Assisted Hydrodistillation: GC-MS Characterization, In Vitro Pharmacological Activities, and Molecular Docking. *Separations* **2024**, *11*, 199. [CrossRef]
26. Rincon, J.; de Lucas, A.; Gracia, I. Isolation of Rock Rose Essential Oil Using Supercritical CO_2 Extraction. *Sep. Sci. Technol.* **2000**, *35*, 2745–2763. [CrossRef]
27. Zhu, K.; Mao, L.; Zhu, X. Studies on supercritical CO_2 extraction of labdanum and its chemical components. *Chem. Ind. For. Prod.* **2004**, *24*, 33–36.
28. Brunner, G. *Gas Extraction*; Steinkopff: Darmstadt, Germany, 1994.
29. McHugh, M.A.; Krukonis, V.J. *Supercritical Fluid Extraction*; Butterworths: Stoneham, MA, USA, 1986.
30. Sovová, H. Rate of the vegetable oil extraction with supercritical CO_2—I. Modelling of extraction curves. *Chem. Eng. Sci.* **1994**, *49*, 409–414. [CrossRef]
31. Sovová, H.; Kučera, J.; Jež, J. Rate of the vegetable oil extraction with supercritical CO_2—II. Extraction of grape oil. *Chem. Eng. Sci.* **1994**, *49*, 415–420. [CrossRef]

32. Langa, E.; Della Porta, G.; Palavra, A.M.F.; Mainar, A.M. Supercritical fluid extraction of Spanish sage essential oil: Optimization of the process parameters and modelling. *J. Supercrit. Fluids* **2009**, *49*, 174–181. [CrossRef]
33. Sovová, H. Mathematical model for supercritical fluid extraction of natural products and extraction curve evaluation. *J. Supercrit. Fluids* **2005**, *33*, 35–52. [CrossRef]
34. Kavoura, D.; Kyriakopoulou, K.; Papaefstathiou, G.; Spanidi, E.; Gardikis, K.; Louli, V.; Aligiannis, N.; Krokida, M.; Magoulas, K. Supercritical CO_2 extraction of *Salvia fruticose*. *J. Supercrit. Fluids* **2019**, *146*, 159–164. [CrossRef]
35. Lemonis, I.; Tsimogiannis, D.; Louli, V.; Voutsas, E.; Oreopoulou, V.; Magoulas, K. Extraction of Dittany (*Origanum dictamnus*) using supercritical CO_2 and liquid solvent. *J. Supercrit. Fluids* **2013**, *76*, 159–164. [CrossRef]
36. Papamichail, I.; Louli, V.; Magoulas, K. Supercritical fluid extraction of celery seed oil. *J. Supercrit. Fluids* **2000**, *18*, 213–226. [CrossRef]
37. NIST Chemistry WebBook. 2023. Available online: https://webbook.nist.gov/chemistry/ (accessed on 2 February 2026).
38. Drosou, C.; Kyriakopoulou, K.; Bimpilas, A.; Tsimogiannis, D.; Krokida, M. A comparative study on different extraction, techniques to recover red grape pomace polyphenols from vinification byproducts. *Ind. Crop. Prod.* **2015**, *75*, 141–149. [CrossRef]
39. Demetzos, C.; Loukis, A.; Spiliotis, V.; Zoakis, N.; Stratigakis, N.; Katerinopoulos, H.E. Composition and Antimicrobial Activity of the essential oil of *Cistus creticus* L. *J. Essent. Oil Res.* **2011**, *7*, 407–410. [CrossRef]
40. Mastino, P.M.; Marchetti, M.; Costa, J.; Usai, M. Comparison of essential oils from *Cistus* species growing in Sardinia. *Nat. Prod. Res.* **2017**, *31*, 299–307. [CrossRef]
41. Abu-Orabi, S.T.; Al-Qudah, M.A.; Saleh, N.R.; Bataineh, T.T.; Obeidat, S.M.; Al-Sheraideh, M.S.; Al-Jaber, H.I.; Tashtoush, H.I.; Lahham, J.N. Antioxidant activity of crude extracts and essential oils from flower buds and leaves of *Cistus creticus* and *Cistus salviifolius*. *Arab. J. Chem.* **2020**, *13*, 6256–6266. [CrossRef]
42. de Pascual Teresa, J.; Urones, J.G.; Marcos, I.S.; Bermejo, F.; Basabe, P. A rearranged labdane: Salmantic acid from *Cistus laurofilius*. *Phytochemistry* **1983**, *22*, 2783–2785. [CrossRef]
43. Pavlić, B.; Bera, O.; Vidović, S.; Ilić, L.; Zeković, Z. Extraction kinetics and ANN simulation of supercritical fluid extraction of sage herbal dust. *J. Supercrit. Fluids* **2017**, *130*, 327–336. [CrossRef]
44. Sovová, H.; Jež., J.; Bártlová, M.; Stastová, J. Supercritical carbon dioxide extraction of black pepper. *J. Supercrit. Fluids* **1995**, *8*, 295–301. [CrossRef]
45. Perakis, C.; Louli, V.; Magoulas, K. Supercritical fluid extraction of black pepper oil. *J. Food Eng.* **2005**, *71*, 386–393. [CrossRef]
46. Roy, B.C.; Goto, M.; Hirose, T.; Navaro, O.; Hortacsu, O. Extraction rates of oil from tomato seeds with supercritical carbon dioxide. *J. Chem. Eng. Jpn.* **1994**, *27*, 768–772. [CrossRef]
47. Maggi, F.; Lucarini, D.; Papa, F.; Peron, G.; Dall' Acqua, S. Phytochemical analysis of the labdanum-poor *Cistus creticus* subsp. eriocephalus (Viv.) Greuter et Burdet growing in central Italy. *Biochem. Syst. Ecol.* **2016**, *66*, 50–57. [CrossRef]
48. Raus de Baviera, D.; Ruiz-Canales, A.; Barrajón-Catalán, E. *Cistus albidus* L.—Review of a Traditional Mediterranean Medicinal Plant with Pharmacological Potential. *Plants* **2023**, *12*, 2988. [CrossRef]
49. Tian, M.; Zhao, X.; Wu, X.; Hong, Y.; Chen, Q.; Liu, X.; Zhou, Y. Chemical Composition, Antibacterial and Cytotoxic Activities of the Essential Oil from *Ficus tikoua*. *Bur. Rec. Nat. Prod.* **2020**, *14*, 219–224. [CrossRef]
50. Guimarγes, R.; Barros, L.; Carvalho, A.M.; Sousa, M.J.; Morais, J.S.; Ferreira, I.C.F.R. Aromatic plants as a source of important phytochemicals: Vitamins, sugars and fatty acids in *Cistus ladanifer*, *Cupressus lusitanica* and *Eucalyptus gunnii* leaves. *Ind. Crops Prod.* **2009**, *30*, 427–430. [CrossRef]
51. Kumar, D.G.; Karthik, M.; Rajakumar, R. GC-MS Analysis of bioactive compounds from ethanolic leaves extract of *Eichhornia crassipes* (Mart) Solms. and their pharmacological activities. *Pharma Innov.* **2018**, *7*, 459–462.
52. Tiji, S.; Rokni, Y.; Benayad, O.; Laaraj, N.; Asehraou, A.; Mimouni, M. Chemical Composition Related to Antimicrobial Activity of Moroccan *Nigella sativa* L. Extracts and Isolated Fractions. *Evid. Based Complement. Altern. Med.* **2021**, *2021*, 8308050. [CrossRef]
53. Bayram, I.; Decker, E.A. Underlying mechanisms of synergistic antioxidant interactions during lipid oxidation. *Trends Food Sci. Technol.* **2023**, *133*, 219–230. [CrossRef]
54. Peyrat-Maillard, M.N.; Cuvelier, M.E.; Berset, C. Antioxidant activity of phenolic compounds in 2,2′-azobis (2-amidinopropane) dihydrochloride (AAPH)-induced oxidation: Synergistic and antagonistic effects. *J. Am. Oil Chem. Soc.* **2003**, *80*, 1007–1012. [CrossRef]

Disclaimer/Publisher's Note: The statements, opinions and data contained in all publications are solely those of the individual author(s) and contributor(s) and not of MDPI and/or the editor(s). MDPI and/or the editor(s) disclaim responsibility for any injury to people or property resulting from any ideas, methods, instructions or products referred to in the content.